

Mobility of long-runout rock flows: a discrete numerical investigation

L. Staron

CNRS-Université Pierre et Marie Curie, Paris VI, Institut Jean le Rond d'Alembert, 4 place Jussieu, case 162, 75252 Paris Cedex 5, France.
E-mail: staron@lmm.jussieu.fr

Accepted 2007 September 23. Received 2007 August 2; in original form 2007 February 7

SUMMARY

In the perspective of studying the mobility and deposit geometry of long-runout flows, discrete numerical simulations of model granular avalanches over simple topography are performed. Analysing the behaviour of the ratio H/L depending on the parameters varied in the simulations, we show its poor sensitivity to the topographic parameters, namely the initial height of the flowing mass and the slope. On the contrary, a correlation between H/L and the frictional properties of the material is established. However, the existence of variations of the effective friction induced by the dynamics are not reflected by the value of H/L . As an alternative to the H/L description of the flow behaviour, we propose a new scaling for the runout distance taking into account the lateral extension L_0 of the relief. Forming the normalized runout L/L_0 , and defining the aspect ratio a of the topography, we show the dependence of L/L_0 on a , thus generalizing previous analysis of Martian data. Analysing the correlation between the normalized runout and the front velocity for the numerical simulations, we show how L/L_0 depends both on the frictional properties of the material *and* on the dynamics of the flow. This result suggests the necessity of evaluating the lateral extension of the relief L_0 in the case of natural flows, in order to define a 'horizontal travel index' including the topography in an attempt to better understand the flow dynamics. Analysing the deposit for both simulations and real flow data we evidence a common behaviour suggesting that the geometric factors prevail in the spreading dynamics irrespective of the details of the flow context and conditions. We moreover assert the relevance of discrete simulations to the discussion of real cases.

Key words: Numerical solutions; Fracture and flow; Friction.

1 INTRODUCTION

In spite of the quantity of research dedicated to rock avalanches and more generally dry debris flows, the behaviour of those remarkable geological events remains a debatable and challenging issue. More specifically, the high mobility characterizing them and allowing the material to reach unexpectedly long runouts is so far essentially unexplained. While different mechanisms were proposed to account for this mobility, involving either fluidization by trapped air (Kent 1966; Shreve 1966) or by acoustic energy (Melosh 1979), lubrication by melted material (Erismann 1979) or more simply by a basal shear layer (Campbell 1989), none of them has been universally acknowledged as being fundamental in the dynamics of long-runout dry flows. An important obstacle for identifying the mechanisms of lubrication or fluidization is the suddenness and destructive power of geological flows which prevent monitoring and direct measurements. As a result, the corpus of data available mainly consists of accurate descriptions of the deposits. However, relating the shape of the deposit to the physical properties of the flow is not straightforward. Accordingly, the evaluation of the mobility can hardly be more than a crude geometrical characterization. Meanwhile, the great va-

riety of material involved, the various triggering mechanisms and the differences in topography severely complicate attempts of generalization. In this context, little is known about dry flows mobility. The simplest approach to evaluate the latter is to identify it with the ratio of the initial height to the final runout distance, relying on the assumption that the potential energy initially available is dissipated by friction force along the runout irrespective of the path followed by the material. The effective friction thus quantified tends to obey an inverse correlation with the volume of the flowing material (Heim 1932). However, while this correlation remains unexplained, no other was clearly evidenced which could lay the basis of a physical understanding of flow mobility.

Considering the difficulties of studying real natural phenomena, simple models of granular flows are expected to bring important insights (Cleary 1993; Campbell 1995; Hutter & Kock 1995; Straub 1997; Hungr & Evans 2004). In this spirit, laboratory experiments of the collapse of columns of grains onto horizontal planes have brought forward a new scaling law for the runout distance (Balmforth & Kerswell 2004; Lajeunesse *et al.* 2004; Lube *et al.* 2004). This scaling only involves the aspect ratio of the initial column before collapse, and is robust against the column volume, the

grains properties and the nature of the substrate. Very interestingly, this scaling law could be successfully confronted with Martian data, and the landslides of Valles Marineris proved to behave in a way similar to the laboratory columns (Lajeunesse *et al.* 2006). However, these results cannot be easily applied to other landslides for which the aspect ratio of the initial mass prior to the flow is difficult to evaluate, and for which topography is likely to play a role. Yet, it seems reasonable to assume that similar scaling could be evidenced in the general case of a granular mass flowing over a simple relief.

In the perspective of studying the runout and deposit of dry flows in relation to simple scalings as observed in (Lajeunesse *et al.* 2006), discrete numerical simulations of model granular avalanches over simple topography are performed. The objective of this investigation is twofold. We first investigate whether the scaling shown in (Lajeunesse *et al.* 2006) can be generalized, and whether it can be related to the frictional properties of the flow, its dynamics and the characteristics of the final deposit. Meanwhile, we question the significance and relevance of the ratio H/L as a quantification of the flow mobility. Then, systematically confronting our results to real flow data, we discuss the reliability of discrete numerical simulations to study geological cases.

The numerical method applied for this study is the non-smooth contact dynamics (Moreau 1994), which proved to reproduce accurately the behaviour of simple granular systems when confronted to laboratory experiments (Staron & Hinch 2005). We are thus confident that the results presented hereafter are a realistic picture of the behaviour of model granular flows. Details of the algorithm and of the numerical setup are presented in Section 2. At this stage, comparison with Martian (Quantin *et al.* 2004) and terrestrial (Nicoletti & Sorriso-Valvo 1991) data allow us to check that simulations are relevant to the discussion of real cases.

Characterizing the mobility of the flow is the subject of Section 3. We show the poor sensitivity of the ratio H/L to the topographic parameters, namely the initial height of the flowing mass and the slope. Alternatively, we propose in Section 4 a new scaling for the runout taking into account the topography and generalizing the scaling observed in (Lajeunesse *et al.* 2006). Analysing the front dynamics in Section 5, we show that the new runout scaling is tightly related to the flow dynamics as well as to the frictional properties of the material. Evaluating an effective coefficient of friction μ_e from the work actually performed by the grains, we establish a correlation between μ_e and H/L . Meanwhile, we give evidence of variations in μ_e induced by the dynamics, hence not reflected by H/L . Analysing the shape of the deposit for both simulations and real flow data in Section 6, we evidence a common behaviour suggesting that the geometric factors prevail in the spreading dynamics irrespective of the details of the flow context and conditions. This suggests the first order role of geometric factors in flow behaviour. We moreover assert the relevance of discrete simulations to the discussion of real cases. The results are discussed in Section 7.

2 THE NUMERICAL EXPERIMENT

2.1 Algorithm and setup

Using the contact dynamics algorithm (Moreau 1994), we simulate the flow of 2-D rigid circular grains interacting through collisions and long-lasting contacts. The grains size is uniformly distributed in an interval such that the ratio of the maximum to the minimum diameter is 1.5. This slight size dispersity prevents the grains from

obeying the unrealistic limit case of crystal-like geometrical ordering. However, it is not sufficient to discuss the influence of size segregation onto flow dynamics. In the following, D denotes the mean grains diameter ($D = 0.05$ m).

The contact dynamics explicitly models the behaviour of each individual grains following the classical equations of the dynamics. The interactions between the grains consists of a simple Coulomb friction law involving the coefficient of intergrain friction μ , and of a hard-core repulsion law. Energy exchanges during collisions are controlled by a Newton coefficient of restitution e . While μ and e are microscopic parameters characteristic of the contact scale, they control the ability of the flow to dissipate its energy at a macroscopic scale. Numerical experiments performed using contact dynamics (Staron & Hinch 2007) have shown that the influence of the value of e is very weak as long as e remains smaller than 0.8; for larger values, clouds of bouncing grains form, and we no longer are in the case of dense granular flows. Hence in the simulations presented in the following, e was set to 0.5 and its influence was not studied. Varying the dissipative flow properties was achieved by changing the value of the intergrain friction μ , which was set alternatively to 0.01, 0.1 and 0.5. No interstitial fluid is considered at all, which implies that any effect of trapped air cannot be accounted for. Moreover, our simulations being 2-D, 3-D effects such as channelization or on the contrary lateral spreading are off discussion. The reliability of the contact dynamics to reproduce the behaviour of 2-D simple granular materials was tested against laboratory experiments involving sand, rice or glass beads. In the case of the column collapse experiment for instance, in which a mass of grains was allowed to spread and flow as a response to gravity, the scaling laws obtained experimentally and numerically were identical, as well as the dynamics of the flow; any differences could be attributed to the properties of the material: friction μ , restitution e and to a smaller extent, the shape of the grains (Staron & Hinch 2005).

The initial mass consists of a rounded heap of lateral width l_m and height h_m obtained by deposition of grains under gravity, and counting N_g grains. While the number of grains was varied from 688 to 6251, the shape of the initial mass was kept unchanged, namely l_m/h_m is constant and equal to 3. The topography over which the granular mass is allowed to flow is made of a circular ramp of radius of curvature R_0 followed by a horizontal plane. The whole length of the topography is made rough by gluing grains of diameter D with the same properties μ and e as the free grains. Alternatively, further simulations were performed where the circular ramp was left smooth in order to observe qualitatively the influence of roughness on the runout. This setup is in the following referred to as *partial roughness*. In any case no erosion processes is made possible. The topography is characterized by the height H_0 and the lateral extension L_0 , and the initial slope θ_0 (see scheme in Fig. 1), thus obeying the following geometrical relations $L_0 = R_0 \sin \theta_0$ and $H_0 = R_0(1 - \cos \theta_0)$.

The initial height of the mass is denoted H , and corresponds to the initial position of the gravity centre. After the mass has flown down the topography and come to a rest, the farthest point of the deposit to the initial position of the front flow defines the lateral extension L , referred to as *runout distance* in the following. The evaluation of L is done practically by excluding the particles rolling ahead independently of the main flow, and takes into account the coherent mass of touching grains only. It should be noted that different definitions are possible for the determination of both H and L , depending on if one considers the initial position of the flow front, the initial position of the centre of mass, or the topmost point of the mass. While choosing H from the initial position of the centre of mass seems logical as it scales like the initial potential energy, the definition of L adopted in

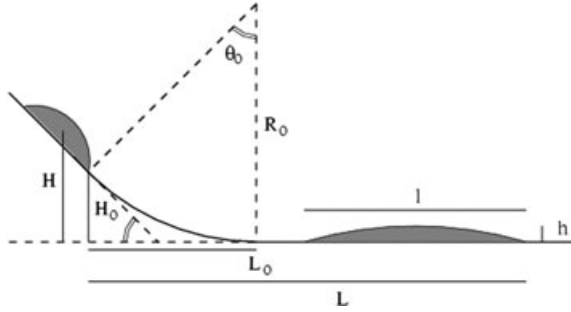


Figure 1. Schematic illustration of the numerical setup. The topography is characterized by the initial slope θ_0 and the initial height H_0 , defining its radius of curvature R_0 . The initial position of the granular mass and the final deposit are both represented, defining the initial height H and the runout distance L . The final deposit is characterized by its lateral extension l and its depth h .

this paper is arbitrary. We have checked however that this choice is of no consequence on the results discussed hereafter.

Several runs were carried out varying independently H_0 , θ_0 , N_g and μ . In addition, few simulations were performed changing the value of the gravity and the substrate roughness. The Table 1 shows the successive series of simulations performed and discussed in this paper with the value of the corresponding parameters. The aim in varying such a large number of parameters is to check if we are able to reproduce the scattering observed in nature; however, the influence of only part of them will be quantitatively and systematically investigated in the following.

Illustration of a simulation is displayed in Fig. 2, where four successive snapshots of the granular mass flowing over the topography are represented together with the time-evolution of the grains mean velocity.

2.2 Comparison with terrestrial and Martian cases

The use of 2-D discrete simulation to study long-runout landslides proceeds from the assumption that in spite of important simplifications, the flow of model granular material under gravity presents essential features which keep a first-order role in real flows. Accordingly the final deposit left by the flow is expected to share a common geometry in simulations and in nature. In order to check the validity of this assumption, we confront the simulations to real flows data. A set of 40 terrestrial rock-avalanches compiled in (Nicoletti & Sorriso-Valvo 1991), together with a set of 45 Martian landslides compiled in (Quantin *et al.* 2004), allow us for a systematic comparison with the geometrical characteristics of the numerical flows.

Comparing real 3-D data with 2-D numerical data requires that quantities should be systematically normalized so as to have the same dimension. This is basically done by introducing in the nor-

malization the rescaled volume $V^{1/d}$, where $d = 2$ or 3. The underlying assumption is that 2-D and 3-D cases do not differ essentially. More specifically, we suppose that the spreading in the third direction in real 3-D cases does not significantly alter the dynamics of spreading in the flow direction. In the same way, 2-D grains having less neighbours than 3-D ones, hence less contacts, they dissipate less efficiently their energy than a collection of real 3-D beads, but exhibit similar dynamics. Altogether, the differences induced by the dimension remain limited.

To compare the range of values taken by the runout considering the volume involved and the initial height of the material for numerical, Martian and terrestrial cases, the variation of the effective friction H/L as a function of the non-dimensional ratio $V^{1/d}/L$ is plotted in Fig. 3(a) (where d is the dimension, that is, 3 for Martian and terrestrial flows and 2 for numerical flows). All series of simulations listed in 1 are reported. The corresponding error bars are smaller than the size of the symbol used, and will not be reported all through the paper. We observe that the numerical points fall in the same cloud of values as the data points, asserting that the simulations are relevant for at least the geometrical aspects of the problem. Moreover, we reproduce a scattering similar to what is observed in nature, and induced by the variations of the topography, the material properties and the volume of the flowing mass; their influence is visible in Fig. 3(b), where the different series of simulation are distinguished. Numerically, the parameter whose influence on H/L is the greatest is the intergrain friction μ . For $\mu = 0.5$ the dissipation becomes very efficient so that we are hardly in the case of long-runout flow. On the contrary for $\mu = 0.1$ and 0.01, the value of H/L obtained is similar to what can be commonly observed in nature. We can as well identify the influence of the roughness of the topography, which significantly increases the dissipation. These aspects however will not be further discussed in the following. We will rather focus on the influence of the geometry, namely the initial height H_0 and the initial slope θ_0 , and the volume of the flowing mass. Their effect on the ratio H/L is the subject of next section.

3 FLOW RUNOUT AND EFFECTIVE FRICTION

3.1 Is H/L a relevant characterization?

The main difficulty arising when trying to understand the dynamics of long-runout dry flows is to draw energy balance from the deposit features. Although the surface area A covered by the flow was shown to be a valuable information for stress and thus dissipation evaluation (Dade & Huppert 1998; Iverson *et al.* 1998), the commonest way of evaluating flow dissipative properties remains the ratio H/L , namely the ratio of the initial height of the mass to the runout distance. From a purely geometrical argument, and in the absence of any decisive effect induced by the topography, it can

Table 1. Series of simulations performed. The intergrain friction μ , the number of grains N_g , the initial height H_0 and slope θ_0 of the topography, the roughness and the gravity are alternatively varied (see text for details).

Series	μ	N_g	H_0 (m)	θ_0 (deg)	Roughness	g (m s ⁻²)	Number of runs
A	0.1	5016	12, 18, 24, 30	$\in [15, 85, 5]$	Yes	9.81	60
B	0.01	5016	12, 24	$\in [15, 85, 5]$	Yes	–	30
C	0.5	5016	18, 30	$\in [15, 85, 5]$	Yes	–	30
D	0.5	688, 1201, 1963	12, 18, 24	$\in [15, 85, 5]$	Partial	–	60
	–	2775, 3718, 4340	–	–	–	–	–
	–	5016, 6251	–	–	–	–	–
E	0.1	5016	12	$\in [30, 80, 10]$	Yes	3.7	6



Figure 2. Example of the flow of a granular mass counting 5016 grains over a rough ramp of initial height $H_0 = 12$ m and initial slope $\theta_0 = 60^\circ$, and with intergrain friction $\mu = 0.1$. Four successive snapshots are represented on the same picture on the left, differentiated by the grey scale used for the grains, black corresponding to initial and final state. The right-hand side picture shows the corresponding normalized mean velocity of the grains as a function of the normalized time, with the dashed vertical lines coinciding with the intermediate grey snapshots of the left-hand side picture.

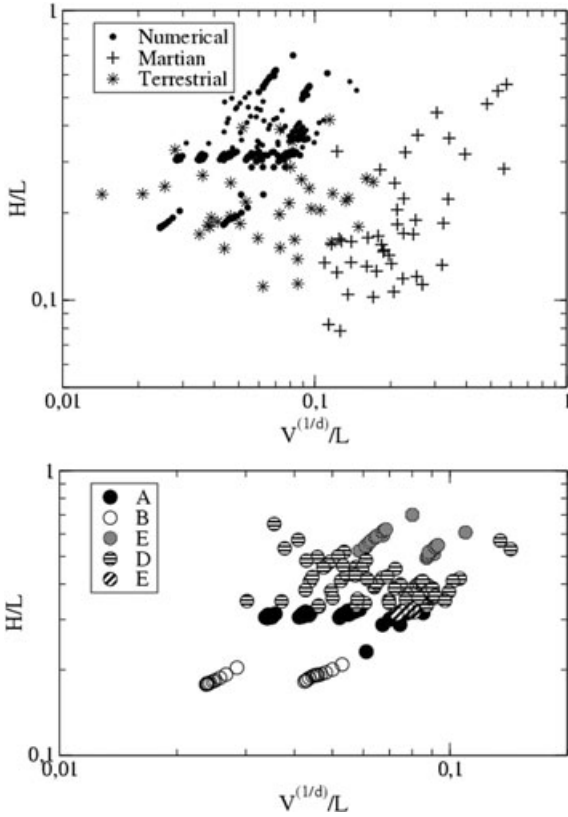


Figure 3. Plot of the effective friction H/L as a function of the non dimensional ratio $V^{1/d}/L$, (a) where $d = 2$ for numerical data, and $d = 3$ for Martian (Quantin *et al.* 2004) and terrestrial (Nicoletti & Sorriso-Valvo 1991) data, and (b) where $d = 2$, for the different series of numerical simulations (see Table 1).

be argued that the area covered by the flow and the runout distance are somewhat correlated, so that the use of L instead of A is not necessarily a misrepresentation. For instance, Fig. 4 shows a clear correlation between non-dimensional runout and surface area in the case of Martian and terrestrial slides (in spite of the non-negligible dispersion of the data). However, identifying H/L with the effective friction raises the problematic issue of the role of the path followed by the flow. Indeed, writing

$$mgH = \mu_e mgL, \quad (1)$$

$$\frac{H}{L} = \mu_e, \quad (2)$$

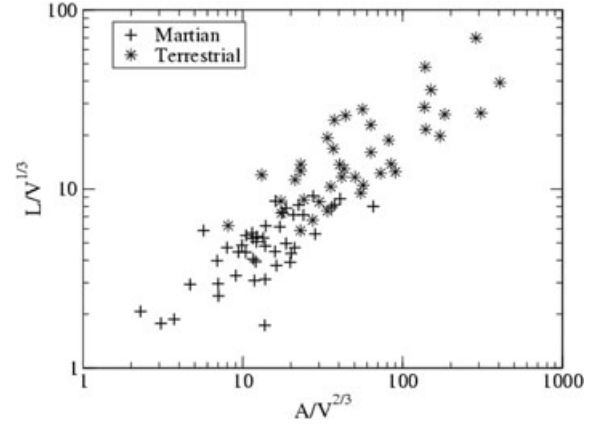


Figure 4. Non-dimensional runout distance $L/V^{1/3}$ as a function of the non-dimensional surface area covered by the flow $A/V^{2/3}$, where V is the volume of the flowing material, for terrestrial (Nicoletti & Sorriso-Valvo 1991) and Martian flows (Quantin *et al.* 2004).

where m is the mass of the flowing material and μ_e the associated coefficient of friction, proceeds from the assumption that the whole initial potential energy is left available for the horizontal flow, regardless of the topography, namely regardless of the details of the work actually performed by the flowing material. It seems however likely that these details are part of the mechanisms where by potential energy is converted efficiently into lateral motion. Accordingly, one would expect the measure of the effective friction to be sensitive to the conditions of the flow. Eventually, the key question is whether the ratio H/L is a relevant characterization of the flow mobility.

In the following, we discuss the sensitivity of H/L to the volume of the flow and to the topography.

3.2 Volume control

An aspect much discussed but poorly established is the sensitivity of the ratio H/L to the volume V of the flowing mass, known as the Heim dependence (Heim 1932). Although the subject of a lively debate, this correlation has however found so far no physical ground. Using numerical run from series D of the simulations (see Table 1), we form the ratio H/L for avalanches involving from few hundredths to few thousands of grains N_g . The resulting dependence is plotted in Fig. 5 for different initial heights H_0 , and for a fixed initial slope θ_0 . We observe a clear diminution of H/L with the number of grains, namely the volume of the avalanche, in agreement with the Heim law. The range of values over which both H/L and N_g vary is too

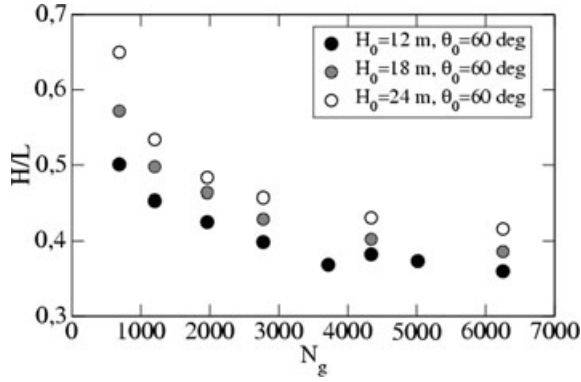


Figure 5. Ratio H/L as a function of the number of grains N_g involved in the avalanches for $H_0 = 12, 18$ and 24 , and $\theta_0 = 60^\circ$ (series D of simulations).

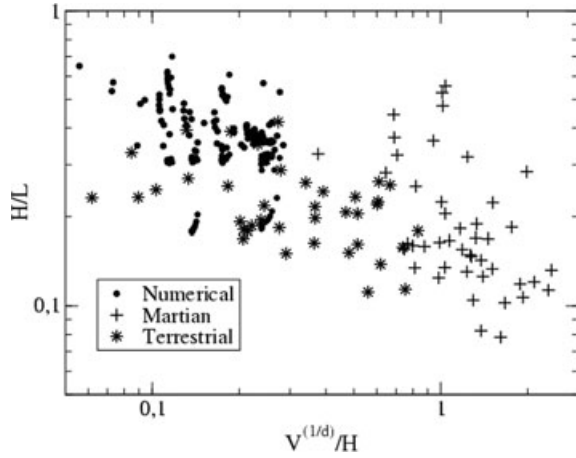


Figure 6. Ratio H/L as a function of the normalized volume $V^{1/d}/H$, with $d = 2$ for numerics and $d = 3$ for terrestrial (Nicoletti & Sorriso-Valvo 1991) and Martian (Quantin *et al.* 2004) data. Numerical points represent all the simulations listed in Table 1.

narrow to be compared with geological scale; however, normalizing the volume of the avalanche using the initial height H for numerical, Martian and terrestrial data, we observe that the simulations behave in a way compatible with the geological cases (Fig. 6).

The dependence of H/L on the volume will not be further discussed in the present contribution, but will be the subject of a forthcoming work.

3.3 Topographic control

To check the effect of the topography on the value of H/L , we focus on the series A of the simulations (see Table 1), namely we do consider variations of H and θ_0 only without introducing variations of material properties, volume, topography roughness or gravity. From Fig. 7(a), we observe that the initial slope θ_0 of the topography plays a negligible role in the values taken by H/L . In the same way, Fig. 7(b) shows the poor influence of the initial height of the flowing material. For comparison, the influence of H on H/L for Martian and terrestrial flows is displayed in Fig. 7(c): no obvious correlation can be seen. It thus seems that the topography only poorly affects the values of H/L . As implicitly presumed in eq. (2) and established by (Heim 1932), H/L is mostly independent on the path followed by the flowing material.

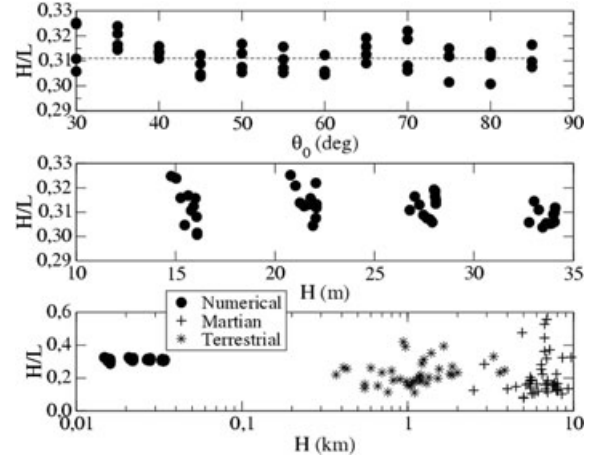


Figure 7. Variations of the ratio H/L for numerical simulations (series A in Table 1): (a) as a function of the initial slope θ_0 , (b) as a function of the initial height H , (c) as a function of H compared with terrestrial (Nicoletti & Sorriso-Valvo 1991) and Martian (Quantin *et al.* 2004) data.

4 THE RUNOUT SCALING LAW

The fact that the ratio H/L is ‘blind’ to the topography implies that it does not reflect at all the dynamics of the flow, that is, the process through which the initial potential energy is converted into spreading. Yet, the collapse experiments (Balmforth & Kerswell 2004; Lajeunesse *et al.* 2004; Lube *et al.* 2004) suggest that this energy transfer plays an important role in the control of the runout distance. In these experiments, the scaling obeyed by the runout was shown to be only dependent on the column initial aspect ratio, and to coincide with the way the vertical acceleration of the falling grains was re-injected in lateral spreading (Staron & Hinch 2005). Although the flow conditions are quite different from those presented in the present contribution, the collapse experiment still suggests that the runout distance is correlated with the way initial potential energy is made available to lateral spreading.

Transposed to our case, the aspect ratio of the initial mass l_m/h_m seems no longer a relevant parameter. However, an aspect ratio can be defined for the topography, as the ratio of the initial height over the horizontal distance travelled by the flowing material before it reaches flat ground. Denoting a this aspect ratio related to the topography, we have

$$a = \frac{H}{L_0}. \quad (3)$$

In other words, a is only a function of the initial slope. Moreover, we define the normalized runout as L/L_0 which can be seen as a kind of ‘horizontal travel index’ measuring the relative distance travelled by the flow over flat ground. (As a remark, this quantity can be compared to the ‘excessive travel distance’ defined by (Hsü 1975), save that we do not presume of the properties of the incline over which the mass flows). It thus now seems possible to generalize the scaling law observed in (Balmforth & Kerswell 2004; Lajeunesse *et al.* 2004; Lube *et al.* 2004) and successfully applied to Martian slides (Lajeunesse *et al.* 2006). The variations of L/L_0 as a function of a is reported in Fig. 8 for the series A, B and C of the simulations, for which the number of grains involved is constant (see Table 1). We observe the collapse of the data following a linear dependence:

$$\frac{L}{L_0} = \lambda(\mu)a, \quad (4)$$

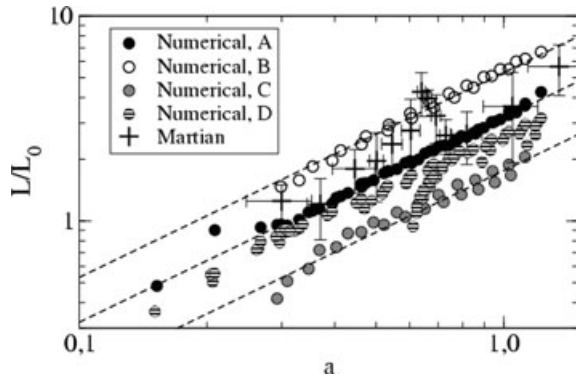


Figure 8. Normalized runout distance L/L_0 as a function of the topography aspect ratio $a = H/L_0$ for the numerical simulations of series A, B, C and D. The dashed line show the linear dependence. The points corresponding to the Martian cliff collapses are taken from (Lajeunesse *et al.* 2006).

where the pre-factor of the linear dependence is a function of the frictional properties of the material, namely function of the value of the intergrain friction μ . We obtain $\lambda(0.1) = 1.76$ in series A, $\lambda(0.01) = 3.2$ in series B and $\lambda(0.5) = 5.3$ in series C. We thus recover the scaling law observed in the collapse experiment (Balmforth & Kerswell 2004; Lajeunesse *et al.* 2004; Lube *et al.* 2004). Note that the scaling (4) can be simply rewritten

$$\frac{L}{L_0} = \frac{L}{H} \frac{H}{L_0} = \frac{L}{H} \times a,$$

which leads directly to

$$\frac{L}{H} = \lambda(\mu).$$

In other words L/H is independent on the topography as observed in previous section, and varies only with the grains properties.

For comparison, the data related to Martian slides and processed by (Lajeunesse *et al.* 2006) are reported in Fig. 8. We observe a very similar behaviour. At this point, one may question the origin of this similarity considering that the Martian scaling account for the initial aspect ratio a of the flowing mass while the numerical scaling (4) accounts merely for the aspect ratio a of the topography. We explain it simply by the fact that in the case of the Martian data, the flow results from cliff collapses, so that the initial aspect ratio of the flowing mass and the topography over which the material flow are intricately related. This is illustrated in Fig. 9. Hence, the aspect ratio defined in (Lajeunesse *et al.* 2006) can easily be interpreted in terms of topography. Inversely, trying to define an aspect ratio for the numerical systems leads us to compare the vertical projection of the sample dimension to its horizontal projection, which is only dependent of the initial slope of the topography, namely of a . It thus appears that the aspect ratio defined in (Lajeunesse *et al.* 2006) and in this work are not essentially different.

Another important difference between the Martian data and the numerical series A, B and C, is that in the latter cases, the volume of the flow is constant, while Martian landslides involve volumes varying between 60 and 9000 km³. To clarify the influence of volume variations on scaling (4), we report the data points from the numerical series D on Fig. 8. We observe that volume variations induce deviations from the linear approximation, but that the latter remains relevant. Moreover, the relative deviations from the linear trend are comparable in the Martian and the numerical case. Certainly a detailed analysis of the influence of volume variation would

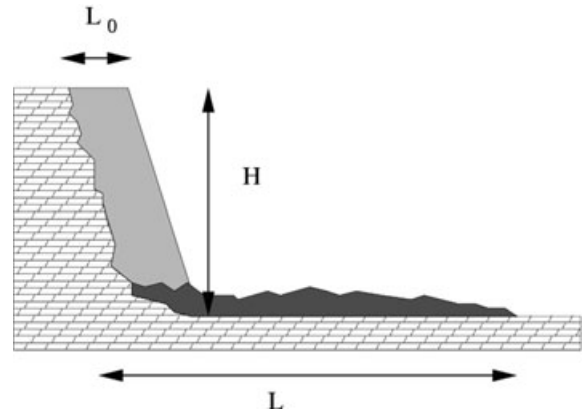


Figure 9. Illustration of the Martian cliff collapse showing how the initial aspect ratio of the flowing mass is directly related to the topography. The dashed area corresponds to the initial position of the mass before collapse. (This illustration being very schematic, the reader should refer to the original paper (Lajeunesse *et al.* 2006) for details on the rigorous way L_0 was determined from the Martian cliff morphology).

be interesting at this point; it is however beyond the scope of this paper. At any rate, the concordance of behaviour between Martian and numerical data is in favour of the generalization of the runout scaling shown in (Lajeunesse *et al.* 2006) to any flow configuration.

Transposed to real flows, this result implies that the description of landslides in terms of runout and initial height is a reflection of the properties of the material only, irrespective of the flow conditions. By opposition, an other important information is the proportion of the runout covered on flat ground, which we expect to be related to the flow dynamics. It implies the evaluation of the lateral extension of the relief whom the flowing mass was initially belonging to, which would give an equivalent of the length L_0 defined in our ideal numerical topography. Although no such measurements are available yet nor such scaling is evidenced in nature, our simulations suggest that the runout scaling is likely to be observed in the case of real geological flows.

Relating the runout scaling to the dynamics of the flow is the subject of the following section.

5 DYNAMICS OF THE FLOW

5.1 The front velocity

In order to filter out the fluctuations induced by the agitation of individual grains, we compute the front velocity v_f as the mean velocity of the grains situated between the front position x_f and the immediately following interval $x_f - 10D$. A example of the evolution of v_f (normalized by the maximum value $v_{f,\max}$ of v_f) as a function of the front position x_f (normalized by L_0) is displayed in Fig. 10, for different values of H_0 and θ_0 . In each case, we observe a period of quick acceleration followed by a slower deceleration. While the influence of the initial angle θ_0 on the final runout is obvious, the curves remains similar one to the other as long as $x/L_0 \leq 1$. We thus assume that the maximum velocity reached by the front $v_{f,\max}$ gives a reasonable estimate of the kinetic energy available for the horizontal runout $L - L_0$ (namely the part of the runout covered on flat ground only) irrespective of the topography. To relate the runout to the flow energy, we plot the normalized horizontal runout $(L - L_0)/L_0$ as a function of $v_{f,\max}^2/(gH)$ for all the simulations (Fig. 11). We observe the collapse of the data following a power

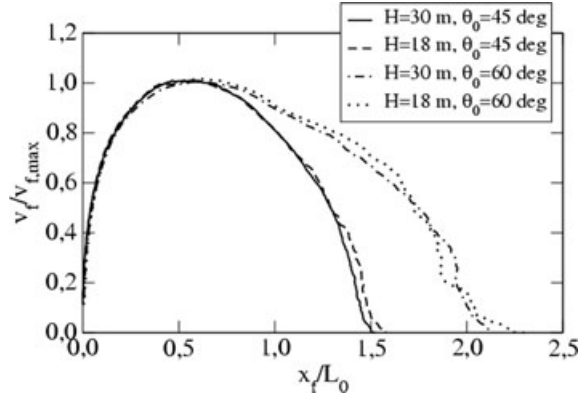


Figure 10. Normalized front velocity $v_f/v_{f,\max}$ as a function of the normalized front position x_f/L_0 for a granular mass counting 5016 grains, a coefficient of intergrain friction of $\mu = 0.1$, and four different configurations of H_0 and θ_0 .

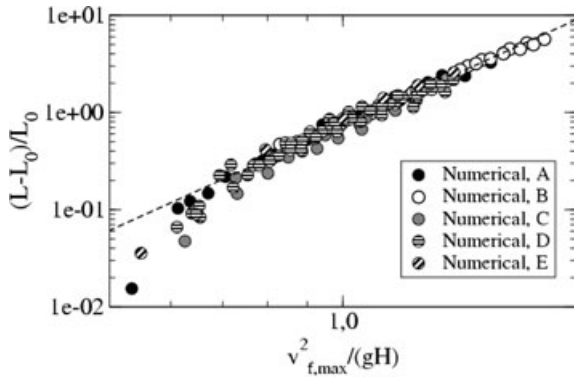


Figure 11. Normalized horizontal runout $(L - L_0)/L_0$ as a function of the normalized maximum kinetic energy of the front $v_{f,\max}^2/(gH)$ for all simulations from series A to series E. The dashed line shows the power-law approximation.

law:

$$\frac{L - L_0}{L_0} = K \left(\frac{v_{f,\max}^2}{gH} \right)^\alpha, \quad (5)$$

with $K \simeq 0.74$ and $\alpha = 3.6 \pm 0.1$, irrespective of all parameters varied in the different series of simulation, namely volume, friction, topography characteristics and roughness, and gravity. This scaling shows how the horizontal runout is at first order dependent only on the proportion of initial potential energy (scaling like gH) made available under the form of kinetic energy (scaling like $v_{f,\max}^2$), this transfer being topography dependent.

As can be seen in Fig. 11, there exists a deviation of the data from the master curve for very low values of $v_{f,\max}^2/(gH)$. In these cases, the flow front stops nearly immediately after reaching flat ground, the greater part of the material remains trapped on the slope, and we are hardly in the case of long runout flows.

5.2 The centrifugal acceleration

Considering the radius of curvature R_0 of the topography, one can expect non-negligible effect due to centrifugal acceleration, denoted g' in the following. If we assume the mean velocity v of the flowing mass to scale like $(gH)^{1/2}$, then $g'/g = v^2/(gR_0)$ scales like $(1 - \cos \theta_0)H/H_0$, that is, like $\simeq (1 - \cos \theta_0)$. In other words, the

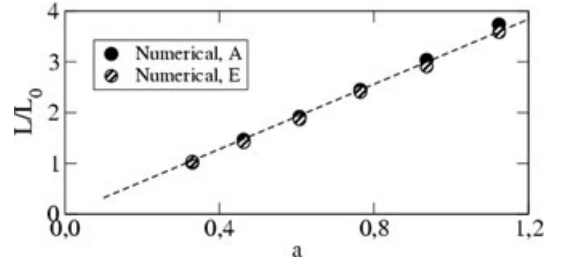


Figure 12. Normalized runout L/L_0 as a function of the topography aspect ratio a for $g = 9.81$ and 3.7 m s^{-2} , all other parameters being the same (series A and E of simulations).

role of centrifugal acceleration becomes non-negligible compared to the role of gravity when the initial slope of the topography is steep enough. One question raised by the possibility of centrifugal acceleration playing a role, is the dependence of rock flows mobility on the absolute value of the gravity g . Indeed, if we stick to the simple friction model as written in eq. (2), we have to include an additional term standing for the centrifugal force which increases the apparent weight of the flowing mass. In other words, we should write, as a crude energy balance:

$$mgH = \mu_e(mg + m v^2/R_0)L, \quad (6)$$

$$\frac{H}{L} = \mu_e \left(1 + \frac{g'}{g} \right), \quad (7)$$

where by the gravity g is no longer simplified out. Since however the simple analysis above predicts that g'/g depends only on the initial slope, the runout should remain independent of g . To check this, we performed a set of simulations with $g = 3.7 \text{ m s}^{-2}$, namely equal to the gravity of mars (series E of simulations). As can be seen in Fig. 12, all parameters beside g being equal, the value of g does not affect the value of the runout beyond the amplitude of error bars, as could be expected. A similar behaviour is expected to hold for real flows.

5.3 Evaluating the effective coefficient of friction

For all simulations, we have access to the position and velocity of each grain in the course of time. Hence, keeping friction as the most likely dissipation process, we can compute an estimation of the effective friction properties of the flow from the details of the work performed by the weight of each grain and the centrifugal force they are subjected to. If we assume that the overall dissipation can be summarized in an effective friction coefficient μ_e , then a possible approximation of the global energy balance is:

$$Ep_0 - Ep_\infty = \mu_e \sum_i \left(\int_{x_{i0}}^{x_{i\infty}} m_i g dx_i + \int_0^{L_0} m_i \frac{v_i^2}{R_0} ds_i \right) \quad (8)$$

where Ep_0 and Ep_∞ are, respectively, the initial and final potential energy of the flowing material, m_i is the mass of the grain i , v_i its velocity, x_{i0} and $x_{i\infty}$ its initial and final position, and where dx_i and ds_i are, respectively, its horizontal and curvilinear incremental displacement (i.e. displacement during a computational time step). Using relation 8, we estimate precisely the value of μ_e for all simulations listed in Table 1 (Note that μ_e is different in meaning and in value from the interparticle friction μ , although dependent on it). We can then relate the runout distance to the actual effective friction properties of the flow.

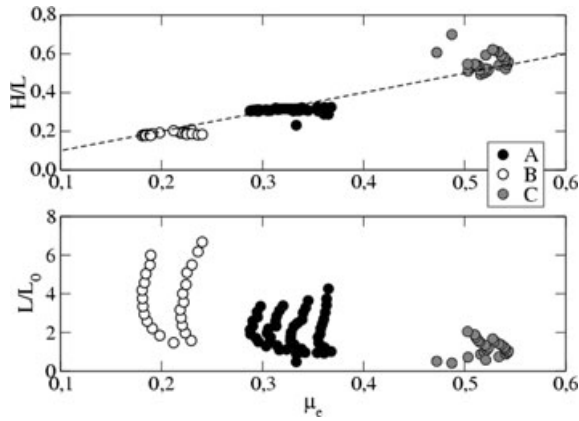


Figure 13. (a) Ratio H/L and (b) normalized runout L/L_0 as a function of the effective coefficient of friction μ_e computed explicitly from grains displacements for simulations series A, B and C. The dashed line in graph (a) shows the approximation $H/L = \mu_e$.

The ratios H/L is plotted as a function of the computed effective friction μ_e in Fig. 13(a) for the simulation series A ($\mu = 0.1$), B ($\mu = 0.01$) and C ($\mu = 0.5$) (see Table 1). We observe the first order equality $H/L = \mu_e$ (represented by a dashed line in Fig. 13a), showing that H/L is indeed a reflection of the friction properties of the material, in agreement with the conclusion drawn in Section 4. However, in each series of simulations, namely for a fixed value of intergrain friction μ but for varying topography, H/L shows no or little variations: as previously established, H/L is essentially ‘blind’ to topography. Moreover, the variations of μ_e in each simulation series show that the effective friction is not only dependent on the properties of the grains, but also on the topography namely on the dynamics of the flow.

The variation of the ratio L/L_0 with μ_e , reported in Fig. 13(b), show no obvious correlation. In the mean, L/L_0 takes smaller values for larger values of μ_e . However, the most apparent feature is the range of values taken by L/L_0 for one given value of μ_e : we observe here the sensitivity of L/L_0 to the variations of the topography.

6 SHAPE OF THE FINAL DEPOSIT

We finally characterize the shape of the deposit through its depth h and its lateral extension l (see Fig. 1). Relating h or l to the dynamics of the flow or to its dissipative properties is very uneasy, and no clear dependence can be evidenced. However, a purely geometrical tendency can be shown between the depth of the deposit and its extension depending on the volume involved in the flow and the initial height of the flowing mass (see Fig. 14). Although rather loose, this correlation nevertheless reflects the role that initial height and flow volume play in the spreading dynamics, even though this role still has to be clarified.

To check whether the correlation observed in Fig. 14 is relevant to real flows, a similar scaling is reported in Fig. 15 for Martian and terrestrial data. In these cases, the extension l of the flow was identified with the runout distance L . The depth h is simply taken as the total volume divided by the surface area of the slide. We observe a similar correlation with a relative collapse of the data compatible with a power law. The numerical points, also reported in Fig. 15, show a behaviour similar to the Martian and terrestrial data (although with a slope slightly smaller).

The conclusion that can be drawn from Fig. 15 is twofold. It first shows that in spite of the differences in context, material and

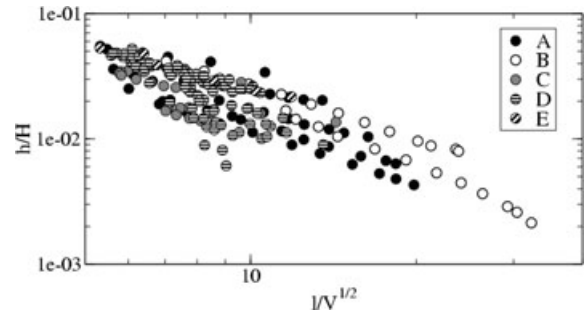


Figure 14. Normalized depth of the flow deposit h/H as a function of its normalized extension $l/V^{1/2}$ for all series of simulations listed in Table 1.

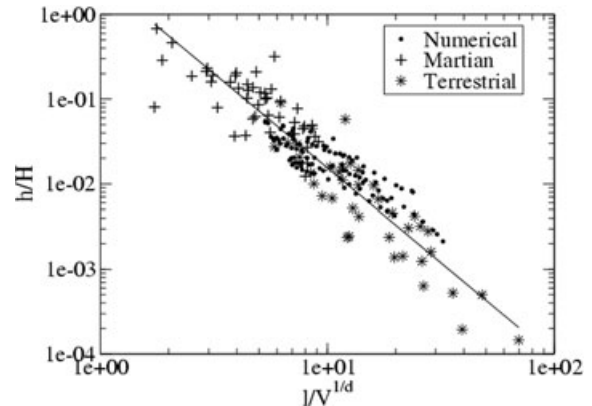


Figure 15. Normalized depth of the flow deposit h/H as a function of its normalized extension $l/V^{1/d}$, where $d = 2$ for numerics and $d = 3$ for data, and where l is taken equal to L for real flows.

topography, the spreading dynamics seems to obey a common organization, depending on the initial height and volume of the flow. This suggests the first order role of the geometry in the flowing behaviour. Then, the agreement between numerical and data point assert the fact that simple 2-D simulations can be relevant to the study of 3-D real cases in spite of the many simplifications.

7 DISCUSSION

In this contribution, we present the results of a discrete numerical study of granular avalanches and their mobility. Different series of simulations were carried out in order to include the influence on the runout of a large number of parameters: grains frictional properties, volume, substrate roughness, gravity and topography, the focus being set on the latter. Meanwhile, systematic comparison between simulations on one hand, and terrestrial and Martian data on the other hand (Nicoletti & Sorriso-Valvo 1991; Quantin *et al.* 2004) allows us to discuss the reliability of our numerical approach, and brings forwards new hypothesis for the behaviour of real flows.

We first analysed the behaviour of the ratio H/L depending on the different factors varied in the simulations. We show its poor sensitivity to the topographic parameters, namely the initial height of the flowing mass and the slope. As well, H/L proves to be independent of the gravity. On the contrary, a correlation between H/L and the frictional properties of the material is established. These three results are in favour of an identification of H/L with the effective friction associated to the flow. However, computing an effective coefficient of friction μ_e from the work actually done by the grains,

we show that this coefficient is sensitive to the topography, namely to the dynamics of the flow. The fact that H/L is independent of the topography implies that it cannot reflect these variations of the effective friction induced by the dynamics.

As an alternative to the H/L description of the flow behaviour, we propose a new scaling for the runout distance taking into account the lateral extension L_0 of the relief, and forming the normalized runout L/L_0 . Considering the aspect ratio a of the topography, we show the dependence of L/L_0 on a , thus generalizing previous analysis of Martian data (Lajeunesse *et al.* 2006). Analysing the correlation between the normalized runout and the front velocity for the numerical simulations, we show how L/L_0 depends both on the frictional properties of the material and on the dynamics of the flow. Accordingly, for one given material, or for materials of similar properties, the ratio L/L_0 only would allow to distinguish and discriminate between various flow occurrences. This result suggests that evaluating the lateral extension of the relief L_0 in the case of natural flows, in order to define a ‘horizontal travel index’ and include the topography in the description of the flow mobility, could help better understanding the flow dynamics. By contrast, the value of H/L should be related to other parameters: volume, static friction, etc.

Finally, analysing the deposit for both simulations and real flow data, we show that relating them to the flow dynamics or frictional properties is not straightforward. Nevertheless we evidence a common behaviour suggesting the existence of a single mechanism prevailing in the spreading dynamics irrespective of the details of the flow context and conditions. This suggests the first order role of geometric factors in flow behaviour. We moreover assert the relevance of discrete simulations to the discussion of real cases.

Although the conclusions drawn in this contribution should be eventually confronted to real flow data, our numerical simulations bring a new insight in the problem of flow mobility by allowing to address quantitatively the role played by the relief, and allowing to investigate the existence of new relevant scaling to flow mobility. One key issue in the problem of long runout flows is the influence of more complex topographic features, as obstacles or abrupt slope transition, as well as fragmentation and erosion of the bed. Each of these aspects should be tackled in relation with the results presented here. One other important aspect is the influence of the volume of the flowing mass, and will be the subject of further work.

ACKNOWLEDGMENTS

The author thanks E. Lajeunesse for kindly providing the Martian landslides data and for stimulating discussion, as well as S. Courrech du Pont, T. H. Druitt and J. C. Phillips are thankfully acknowledged for their critical comments and valuable suggestions on the paper.

REFERENCES

- Balmforth, N.J. & Kerswell, R.R., 2004. Granular collapse in two dimensions, *J. Fluid Mech.*, **538**, 399–428.
- Campbell, C.S., 1989. Self-lubrication for long runout landslides, *J. Geol.*, **97**, 653–665.
- Campbell, C.S., Cleary, P.W. & Hopkins, M., 1995. Large-scale landslide simulations: global deformation, velocities and basal friction, *J. geophys. Res.*, **100**(B5), 8267–8283.
- Cleary, P.W. & Campbell, C.S., 1993. Self-lubrication for long run-out landslides: examination by computer simulation, *J. geophys. Res.*, **98**(21), 911–924.
- Dade, W.B. & Huppert, E.H., 1998. Long-runout rockfalls, *Geology*, **26**(9), 803–806.
- Erismann, T.H., 1979. Mechanisms of large landslides, *Rock. Mech.*, **12**, 5–46.
- Heim, A., 1932. Der Bergsturz Von Elm, *Z. Dtsch. Geo. Ges.*, **34**, 74–115.
- Hungr, O. & Evans, S.G., 2004. Entrainment of debris in rock avalanches: an analysis if a longrunout mechanism, *Geo. Soc. Am. Bull.*, **116**(9/10), 1240–1252.
- Hutter, K. & Koch, T., 1995. The dynamics of avalanches of granular materials from initiation to runout. Part II: experiments, *Acta Mech.*, **109**, 127–165.
- Hsü, K.J., 1975. Catastrophic debris streams (Sturzstroms) generated by rockfalls, *Geol. soc. Am. Bull.*, **86**, 129–140.
- Iverson, R.M., Schilling, S.P. & Vallance, J.W., 1998. Objective delineation of lahar-inondation hazard zone, *Geol. soc. Am. Bull.*, **110**(8), 972–984.
- Kent, P.E., 1966. The transport mechanisms in catastrophic rockfalls, *J. Geol.*, **74**, 79–83.
- Lajeunesse, E., Mangeney-Castelneau, A. & Vilotte, J.-P., 2004. Spreading of a granular mass on an horizontal plane, *Phys. Fluids*, **16**, 2731–2738.
- Lajeunesse, E., Quantin, C., Allemand, P. & Delacourt, C., 2006. New insights on the runout of large landslides in the Valles-Marineris canyons, Mars, *Geophys. Res. Lett.*, **33**, L04403.
- Lube, G., Huppert, H.E., Sparks, R.S.J. & Hallworth, M.A., 2004. Axisymmetric collapses of granular columns, *J. Fluid Mech.*, **508**, 175–199.
- Melosh, H.J., 1979. Acoustic fluidization: a new geological process?, *J. geophys. Res.*, **84**, 7513–7520.
- Moreau, J.-J., 1994. Some numerical methods in multibody dynamics: application to granular materials, *Eur. J. Mech. A-Solids*, **4**, 93–114.
- Nicoletti, P.G. & Sorriso-Valvo M., 1991. Geomorphic controls of the shape and mobility of rock avalanches, *Geol. soc. Am. Bull.*, **103**, 1365–1373.
- Quantin, C., Allemand, P. & Delacourt, C., 2004. Morphology and geometry of Valles Marineris landslides, *Planet. Space Sci.*, **52**, 1011–1022.
- Shreve, R.L., 1966. Sherman landslide, Alaska, *Science*, **154**, 1639–1643.
- Staron, L. & Hinch, E.J., 2005. Study of the collapse of granular columns using two-dimensional discrete-grains simulation, *J. Fluid Mech.*, **545**, 1–27.
- Staron, L. & Hinch, E.J., 2007. The spreading of a granular mass: role of grain properties and initial conditions, *Granular Matter*, **9**, 205–217.
- Straub, S., 1997. Predictability of long-runout landslide motion: implications from granular flow mechanics, *Geol. Rundsh.*, **86**, 415–425.